Carbohydrate Polymers 83 (2011) 883–890

Contents lists available at ScienceDirect

Carbohydrate Polymers

journal homepage: www.elsevier.com/locate/carbpol

Silver nanoparticles encapsulated in glycogen biopolymer: Morphology, optical and antimicrobial properties

D.K. Božanić[a], S. Dimitrijević-Branković[b], N. Bibić[a], A.S. Luyt[c], V. Djoković[a,*]

[a] Vinča Institute of Nuclear Sciences, University of Belgrade, P.O. Box 522, 11001 Belgrade, Serbia
[b] Department of Bioengineering and Biotechnology, Faculty of Technology and Metallurgy, University of Belgrade, Karnegijeva 4, 11120 Belgrade, Serbia
[c] Department of Chemistry, University of the Free State (Qwaqwa Campus), Private Bag X13, Phuthaditjhaba 9866, South Africa

ARTICLE INFO

Article history:
Received 5 May 2010
Received in revised form 17 August 2010
Accepted 31 August 2010
Available online 6 September 2010

Keywords:
Silver nanoparticles
Glycogen
Biopolymer nanocomposites
Antimicrobial activity

ABSTRACT

The glycogen biopolymer from the bovine liver has been used as stabilization agent for the growth of silver nanoparticles. The samples with various contents of silver were prepared by two different procedures that include fast (using microwave radiation) and slow (conventional) heating of the reaction mixtures. The TEM images of the two nanocomposites showed the presence of nanoparticles with average diameter of 9.7 and 10.4 nm, respectively. The results also revealed that the optical properties of the obtained nanocomposite samples strongly depend on the method of preparation. The samples prepared using microwave radiation exhibited narrower surface plasmon resonance peaks, while the silver nanoparticles induced quenching of the photoluminescence of glycogen in all of the tested samples. Antimicrobial activity tests were carried out against *Staphylococcus aureus*, *Escherichia coli* and *Candida albicans* pathogens and showed that the microbial growth was gradually reduced as the concentration of the silver increased. Also, after 2 h of exposure to the nanocomposites the number of cells was significantly reduced (>99%) for all the strains tested.

1. Introduction

Research on integration of polysaccharide biopolymers and inorganic nanoparticles into hybrid systems is witnessing a dramatic activity in current bio-nanoscience. Characteristic macromolecular and supramolecular properties of these biopolymers make them good controlled environments for growth of metallic and semiconductor nanocrystals. Due to a large number of OH groups, polysaccharide chains complexate well with metallic ions in solution, while supramolecular nanostructures formed by inter- and intra-chain hydrogen bonding act as template for nanoparticle growth (Raveendran, Fu, & Wallen, 2003). To date, starch is the most extensively used biopolymer for the stabilization of the growth of metallic (Božanić et al., 2007; Djoković et al., 2009; Raveendran et al., 2003; Sarma & Chattopadhyay, 2004) and semiconductor (Božanić et al., 2007, 2009; Radhakrishnan, Georges, Nair, Luyt, & Djokovic, 2007; Rodriguez et al., 2008; Vigneshwaran, Kumar, Kathe, Varadarajan, & Prasad, 2006) nanoparticles. The other polysaccharide biopolymers such as chitosan (Murugadoss & Chattopadhyay, 2008; Sun et al., 2008; Wei & Qian, 2008), alginate (Pal, Esumi, & Pal, 2005; Brayner, Vaulay, Fievet, & Coradin, 2007), gum Arabic (Kattumuri et al., 2007) or cellulose (Pirkkalainen et al., 2008) also proved to be good stabilization agents. It is also important to mention that nanoparticles synthesized within the biopolymer are biocompatible and hydrophilic, which could be important for their application in biology and medicine. On the other hand, the number of studies in which polysaccharide biopolymers of animal origin were used in preparation of inorganic nanoparticles is limited. In the present study we prepared silver nanoparticles in the presence of a glycogen biopolymer.

Glycogen, the main carbohydrate-storage in animals and microorganisms, is a polysaccharide that consists of highly branched $(1\rightarrow4)(1\rightarrow6)$-linked α-D-glucoses (Manners, 1991). It is produced primarily by the liver and the muscles, but can also be made by glycogenesis within the brain, thymus and skin (Brown, 2004). Glycogen has a high molecular weight (10^6–10^9) and its molecules are packed into spherical granules (β-particles), 20–40 nm in size, which often group together into much larger α-particles. The highly branched, actually fractal (Melendez, Melendez-Hevia, & Canela, 1999), structure of the glycogen enables a very easy pathway of synthesis and degradation as well as simplicity in the regulation mechanism. However, we believe that this dendrimeric structure is also an ideal environment for the controlled synthesis of metallic nanoparticles. The preparation of metal–glycogen hybrid nanostructures could be important from a practical point of view, due to their possible application as probe materials for glucan–biomolecule interactions. Li and co-workers (Xiang, Xu, Liu, Li, & Li, 2009) found, after mixing previously prepared gold nanoparticles and glycogen, that interactions between glycogen and biomacromolecules can alter the aggregation status of

* Corresponding author. Tel.: +381 118066428; fax: +381 113440100.
E-mail address: djokovic@vinca.rs (V. Djoković).

0144-8617/$ – see front matter © 2010 Elsevier Ltd. All rights reserved.
doi:10.1016/j.carbpol.2010.08.070

gold nanoparticles, which produced intensity changes in plasmon resonance light-scattering.

Antimicrobial activity is an important property of silver nanoparticles and/or silver–polymer nanocomposites. A number of studies emerged lately on this subject (Dror-Ehre, Mamane, Belenkova, Markovich, & Adin, 2009; Jain et al., 2009; Kvitek et al., 2008; Lok et al., 2007; Morones et al., 2005; Panacek et al., 2006; Sharma, Yngard, & Lin, 2009), reporting on the influence of different factors, such as the nanoparticle concentration, size and capping agents involved on the inhibition of the antimicrobial growth. It is believed that the antimicrobial activity of silver nanoparticles originates from the formation of Ag^+ active species (Lok et al., 2007), since they exhibit strong affinity towards sulphur and phosphor containing functional groups from the membrane-bound enzymes (McDonnell & Russell, 1999). The accumulation of the nanoparticles in the cells might also be a source of bactericidal activity (Morones et al., 2005). Given that glycogen is a biocompatible polymer of animal origin and that, to our best knowledge, it was not used so far as a stabilization agent for the growth of silver nanoparticles, we considered that it would be interesting from a fundamental as well as from a practical point of view to investigate the antimicrobial effects of this material. The present study is divided into two parts. In the first part, the structure and the optical properties of the silver–glycogen nanocomposites prepared by two different synthetic procedures were investigated. In the second part the antimicrobial activity of the nanocomposite films was tested against the *Staphylococcus aureus*, *Escherichia coli* and *Candida albicans* pathogens.

2. Experimental

2.1. Materials and the preparation of the nanocomposites

2.1.1. Materials

Glycogen from bovine liver, ammonium hydroxide (NH_4OH), D-glucose and silver nitrate ($AgNO_3$) were purchased from Sigma–Aldrich and used as received. High purity water (specific resistance $\sim 10^{18}\ \Omega$ m) was used in all synthetic procedures.

2.1.2. Synthesis of Ag–glycogen nanocomposites

Two different green chemical procedures for the preparation of the nanocomposites were employed:

1. In the first procedure, a modified Tollens method for the preparation of silver nanoparticles was used (Panacek et al., 2006). The silver nanoparticles were synthesized by reduction of $[Ag(NH_3)_2]^+$ ions using D-glucose as a reducing agent in the aqueous glycogen solution and under microwave irradiation. In a typical procedure, a 1 mL of a 0.1 M solution of $AgNO_3$ and 2.5 mL of 0.1 M solution of D-glucose were added to 50 mL of a 0.5% aqueous solution of glycogen. The mixture was stirred for 60 min at room temperature and purged with argon. After that, NH_4OH was added to 5 mL of the obtained solution until pH value reached 8.5. Finally, the mixture was treated in a conventional microwave for 30 s at 440 W. The nanocomposite films were obtained after evaporation of water.
2. The second procedure was a "green" synthetic method reported by Raveendran et al. (2003) for the preparation of starch capped silver nanoparticles. In this method Ag–glycogen nanocomposites were prepared by conventional heating on a hot plate. The same initial mixtures as in the previous procedure were purged with argon, sealed, heated to 50 °C and maintained at this temperature for 24 h. Different samples were prepared by changing the initial amount of silver while the nanocomposite films were obtained after solvent evaporation.

Table 1
List of Ag–glycogen nanocomposite samples and the initial amount of chemicals used in their preparation.

Label	n_m ($AgNO_3$) [mM][a]	n_m (D-Glucose) [mM][b]	Ag [wt.%][c]	Treatment
MW-1	0.5	1.25	2	Microwave
MW-2	1.0	2.50	4	Microwave
MW3	2.0	5.00	8	Microwave
HP-1	0.5	1.25	2	Hot plate
HP-2	1.0	2.50	4	Hot plate
HP3	2.0	5.00	8	Hot plate

[a] Silver concentration.
[b] Concentration of D-glucose.
[c] Silver weight fraction in the nanocomposite.

The preparations conditions and the denotations of the samples obtained using these two procedures are given in Table 1. Throughout the discussion the samples prepared by microwave radiation and conventional heating will be referred to as MW and HP samples, respectively.

3. Methods

3.1. Characterization of the nanocomposites

The morphology and dispersion of the Ag nanoparticles in the glycogen matrix were investigated by transmission electron microscopy (Philips CM100 instrument) at a 80 kV operating voltage. A water dispersion of the nanocomposite was deposited on carbon coated (MW3 sample) and formvar coated (HP3 sample) copper grids using a fine pipette. The samples were left to dry in air before they were transferred to the TEM chamber. The distribution of particle sizes was determined by measuring the diameters of the equivalent circular area of 125 (MW3 sample) or 172 (HP3 sample) observed particles. The obtained histograms were fitted by log-normal distribution with parameters D_{LN} (mean) and σ_{LN} (standard deviation).

The surface morphology of the pure glycogen powder and silver–glycogen nanocomposite films (MW3 and HP3 samples) was investigated by scanning electron microscopy (SEM) using a JEOL JSM 6460LV instrument. The images were obtained using both secondary electron and back-scattered electron (BSE) imaging modes. Due to the poor conductivity of the materials, the samples were coated with carbon prior to SEM investigations. Their composition was checked with EDX measurements done with an X-ray microanalysis unit (Oxford Instruments) attached on SEM.

The X-ray diffraction (XRD) measurements of the MW3 and HP3 nanocomposite samples were performed on a Philips PW3710 X-ray diffractometer (Cu radiation, $\lambda = 0.154$ nm).

The UV–vis absorption measurements of the Ag–glycogen solutions were carried out on a Thermo Evolution 600 spectrophotometer.

FTIR spectroscopic analyses of the pure glycogen and the Ag–glycogen nanocomposite films were carried out at room temperature using a Nicolet 380 spectrophotometer in the spectral range of 4000–400 cm^{-1}, with a resolution of 4 cm^{-1}. The datasets were averaged over 200 scans.

The photoluminescence spectra of the pure glycogen and the Ag–glycogen nanocomposite films were recorded using a Perkin–Elmer LS45 fluorescence spectrophotometer.

3.2. Indicator strains and culture conditions

The microorganisms used in this study were Gram-positive bacteria *S. aureus* ATCC 25922, Gram-negative bacteria *E. i* ATCC 25923, and fungus *C. albicans* ATCC 24433. The growth of microorganisms

for investigation was carried out in a Trypton Soy broth or agar, supplemented with 0.6% (v/v) yeast extract (TSYB or TSYA—Institute of Immunology and Virology, Torlak, Belgrade). A potassium hydrogen phosphate buffer solution (pH 7.0) was used as a liquid medium for quantitative testing of the microbicidal activity of the samples. For inoculum preparation, the microorganisms were cultivated in TSYB at 37 °C and left overnight (late exponential stage of growth). The obtained numbers of *S. aureus*, *E. coli* and *C. albicans* in inoculums were 2.1×10^7 CFU mL^{-1}, 2.4×10^7 CFU mL^{-1}, and 4.0×10^6 CFU mL^{-1}, respectively.

3.3. Antimicrobial activity testing

Two methods were used for the determination of the antimicrobial activity of the silver–glycogen nanocomposites. The first screening was performed by the agar-well diffusion method. The study of the cells reduction activity of the silver–glycogen nanocomposites was performed in a liquid buffer system using a colony count method. In addition, the influence of the concentration of the silver–glycogen nanocomposites on their antimicrobial activity was determined.

For the agar-well diffusion method 60 μL of fresh overnight cultures of indicator strains were added in 6 mL of soft TSYA (0.6% of agar–agar in TSYB). The soft agar was vigorously mixed and poured over Petri plates with previously dried TSYA on the surface of which sterile ceramic tubes (7 mm diameter) were placed. After solidification of the soft agar, the tubes were removed and the obtained wells were filled with 50 μL of control and Ag–glycogen aqueous solutions. All plates were incubated at 37 °C for 24 h. The width of the inhibition zones was measured in millimeters. To establish the nature of the inhibitory activity of the silver–glycogen nanocomposites (-cidal or -static), samples were taken from the clear zones with a loop, surface-plated onto TSYA and incubated under optimal conditions for up to 48 h.

The quantitative testing of Ag–glycogen nanocomposite antimicrobial activity was assessed in a potassium hydrogen phosphate buffer solution (pH 7.00). The solutions of given concentration of the pure glycogen and the nanocomposites were placed in glass tubes containing 9 mL of buffer solution inoculated with 1.0 mL of diluted microbial inoculum (1 mL of initial cultures with 9 mL of saline). The resulting mixture with samples was vortexed for 10 s and incubated at 37 °C in a water bath shaker. After 1 and 2 h of exposure, 0.1 mL aliquots were removed and further diluted with sterile physiological saline solution (8.5 g NaCl in 1 L of water). From all dilutions 1.0 mL aliquots were placed in Petri dishes, overlaid with TSYA and after 24 h of incubation at 37 °C, the counts of viable microorganisms were determined. The percentage of microbial cells reduction (R, %) was calculated using the following equation:

$$R,\ \% = \frac{CFU_{cont./Gly} - CFU_{Ag/Gly}}{CFU_{cont./Gly}} \times 100\%, \quad (1)$$

where $CFU_{cont./Gly}$ and $CFU_{Ag/Gly}$ are the numbers of colony forming units per millilitre for respectively the negative control (containing glycogen without Ag) and the Ag–glycogen nanocomposite samples.

The influence of the concentration of Ag–glycogen nanocomposites on their antimicrobial activity was determined on agar plates. The investigated concentrations were 5, 20, 50 and 200 μg mL^{-1}. Samples of given concentration were inserted in 9 mL of molten (45 °C) TSYA. 1 mL of diluted inoculum (10^{-2}) was added and mixture vortexed (20 s) and placed in sterile Petri dish. After solidification of the agar, the plates were incubated for 24 h at 37 °C and the appearance of viable cells was examined.

All experiments were performed in triplicates and the results are shown as mean values.

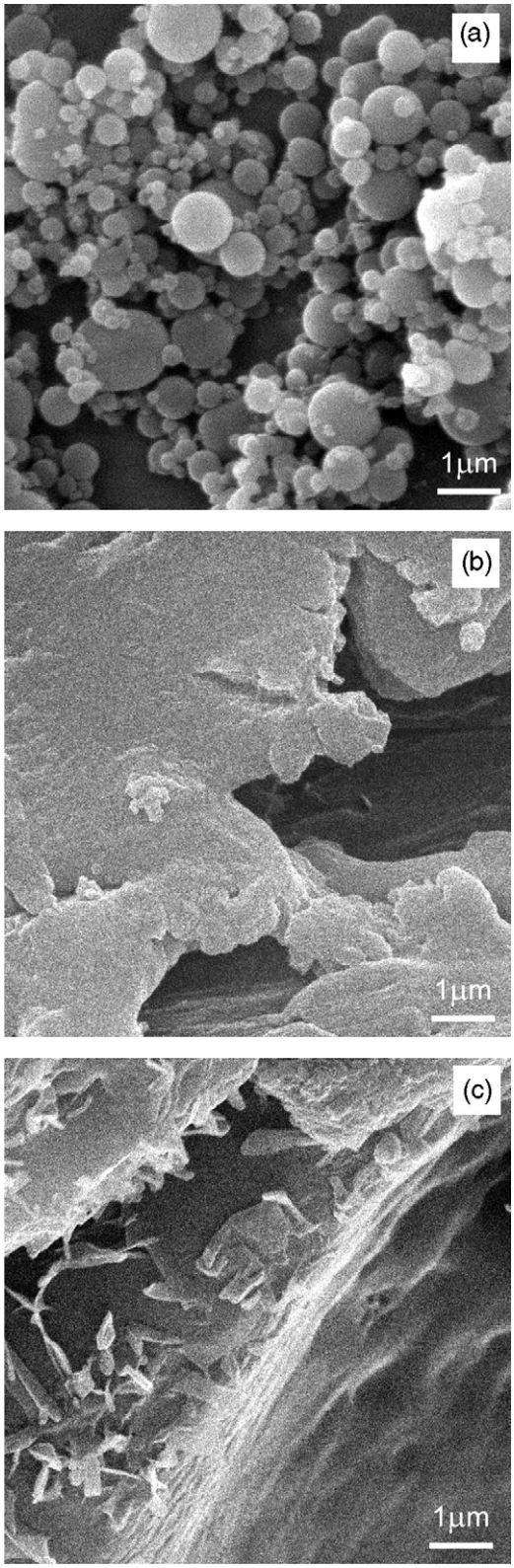

Fig. 1. SEM micrographs of (a) as received glycogen powder and the Ag–glycogen nanocomposite films prepared by (b) MW and (c) HP methods.

4. Results and discussion

4.1. Morphology and structure

Fig. 1 shows the SEM micrographs of the as received glycogen powder and the two nanocomposite films. The image of the neat

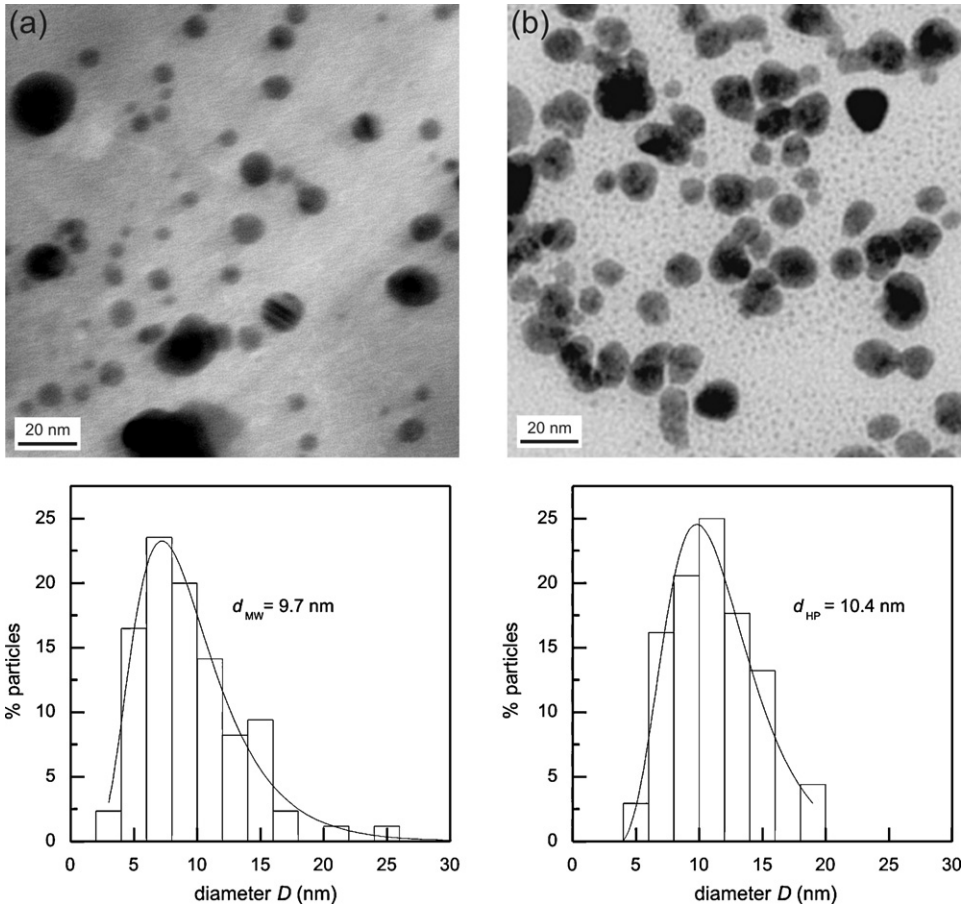

Fig. 2. TEM images of silver–glycogen nanocomposite films prepared by (a) MW and (b) HP methods. Bottom: corresponding size distribution histograms of nanoparticles. The histograms were fitted by a log-normal distribution curve with parameters (a) D_{LN} = 7.2 nm, σ_{LN} = 0.9 and (b) D_{LN} = 9.8 nm, σ_{LN} = 0.7.

glycogen in Fig. 1a depicts spherical α-particles with sizes in the range from several hundred nanometers to approximately 1 μm. After casting of the glycogen–Ag solution into films, the morphology changed. The images in Fig. 1b and c, show that the film surfaces are rough but no particle-like structures were observed. On the other hand, the morphology of the pure glycogen film (not shown) was similar to that of the nanocomposites, which implies that the change in morphology was not due to the presence of the silver nanoparticles.

The TEM micrographs of the nanocomposite films and the corresponding size distribution of the nanoparticles are shown in Fig. 2. It can be seen that the silver nanoparticles are well dispersed in the glycogen matrix. The average sizes of the particles obtained by MW and HP methods are d_{MW} = 9.7 nm and d_{HP} = 10.4 nm (Fig. 2). The size distribution is relatively narrow (the estimated polydispersities are about 50% for MW3 and about 60% for HP3 sample) proving that the glycogen is a good controlled environment for the growth of the metallic nanoparticles.

Fig. 3 shows the XRD spectra of the nanocomposite films. A broad peak at $2\theta \sim 20^{\circ}$ originates from the glycogen matrix while the other two peaks can be assigned to the cubic crystal structure of silver.

4.2. Optical and FTIR spectroscopy

The UV–vis spectra of the Ag–glycogen water solutions prepared by the MW and HP methods are shown in Fig. 4. A surface plasmon resonance (SPR) peak at ~400 nm can be noticed in the spectra of all of the investigated materials. However, depending on the silver content, the nanocomposites prepared using the MW method exhibit somewhat different absorption behavior than those prepared using the HP method. Although increasing of the concentration of the silver in both materials increases the intensity of the SPR-peaks and induce their shift towards lower wavelengths, the resonance peaks of the MW sample are more narrow (Fig. 4). This

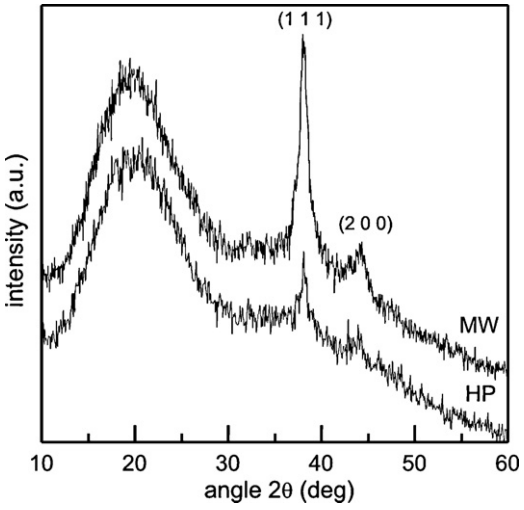

Fig. 3. XRD spectrum of Ag–glycogen nanocomposite films.

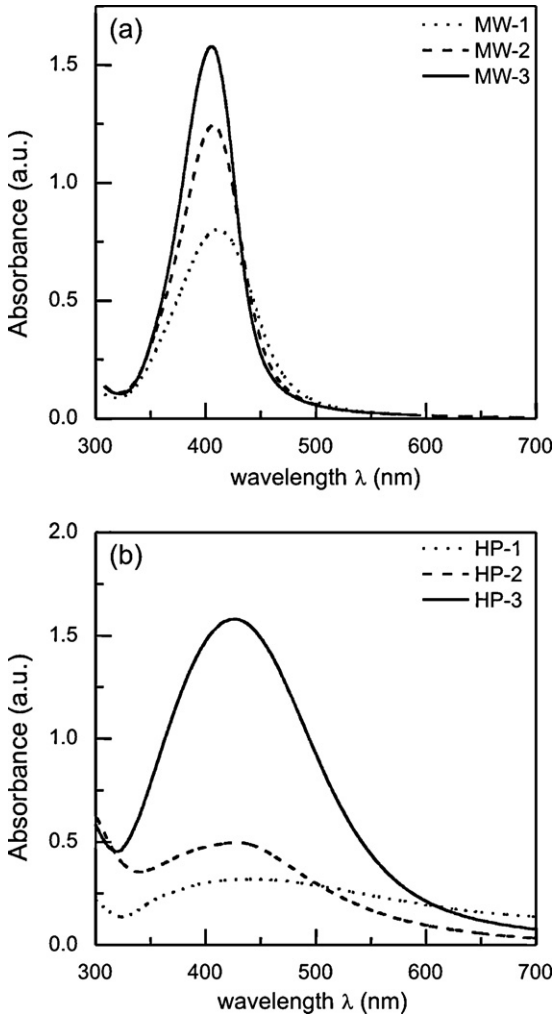

Fig. 4. Absorption spectra of (a) MW and (b) HP silver–glycogen nanocomposite solutions with various silver contents (dotted line (0.5 mM), dashed line (1 mM) and solid line (2 mM)).

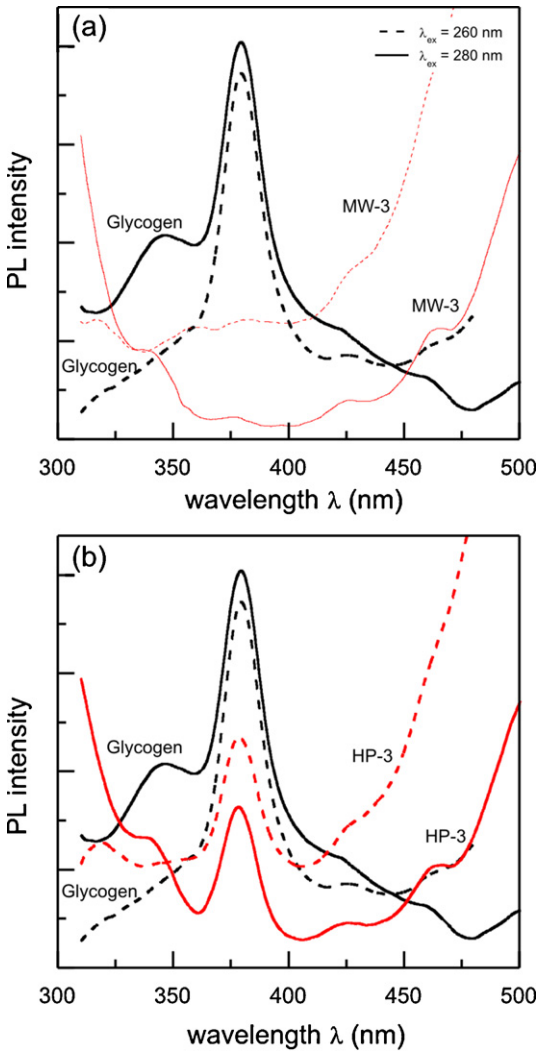

Fig. 5. Fluorescence spectra of the pure glycogen and the Ag–glycogen nanocomposite films prepared by (a) MW and (b) HP methods. The spectra were recorded at two different excitation wavelengths λ_{exc} = 260 nm (dashed lines) and λ_{exc} = 280 nm (solid lines).

is probably a consequence of the narrow size distribution of the nanoparticles in this material. The fast transfer of energy through microwave radiation obviously induces more localized growth of the nanoparticles in the presence of glycogen molecules than in the case of slow heating.

The fluorescence spectra of the pure glycogen and the glycogen–Ag nanocomposites obtained after excitation at 260 and 280 nm are shown in Fig. 5. The main photoluminescence peak of the glycogen is positioned at 380 nm and originates, actually, from the presence of the protein glycogenin (Romero, Carrizo, Montich, & Curtino, 2001). Since silver nanoparticles absorb in the same part of the electromagnetic spectrum (Fig. 4), quenching of the emission was observed for both nanocomposite spectra. However, in the MW sample (Fig. 5a), the emission activity is almost completely destroyed by the presence of the nanoparticles.

The FTIR–ATR spectroscopy measurements were performed in order to study possible interactions between the silver nanoparticles and the glycogen macromolecules. Fig. 6 shows the FTIR spectra of the pure glycogen as well as the MW and HP nanocomposite films. Comparing to the spectrum of the pure biopolymer, there is a change in the spectrum of the nanocomposite in the region 1500–1200 cm^{-1}, which is typical for CH and OH vibrations in alcohols (Socrates, 1994). As a consequence of the particle-macromolecule interaction, the weak modes at 1371 and 1417 cm^{-1} disappears and a strong single mode at 1384 cm^{-1}

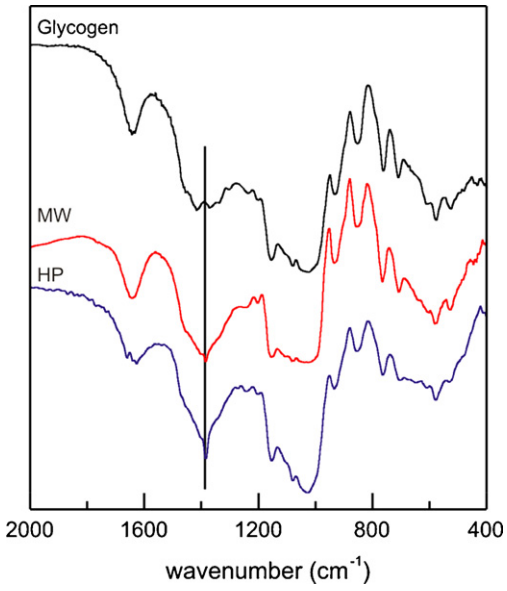

Fig. 6. FTIR spectra of the pure glycogen and Ag–glycogen nanocomposite films prepared by MW and HP methods.

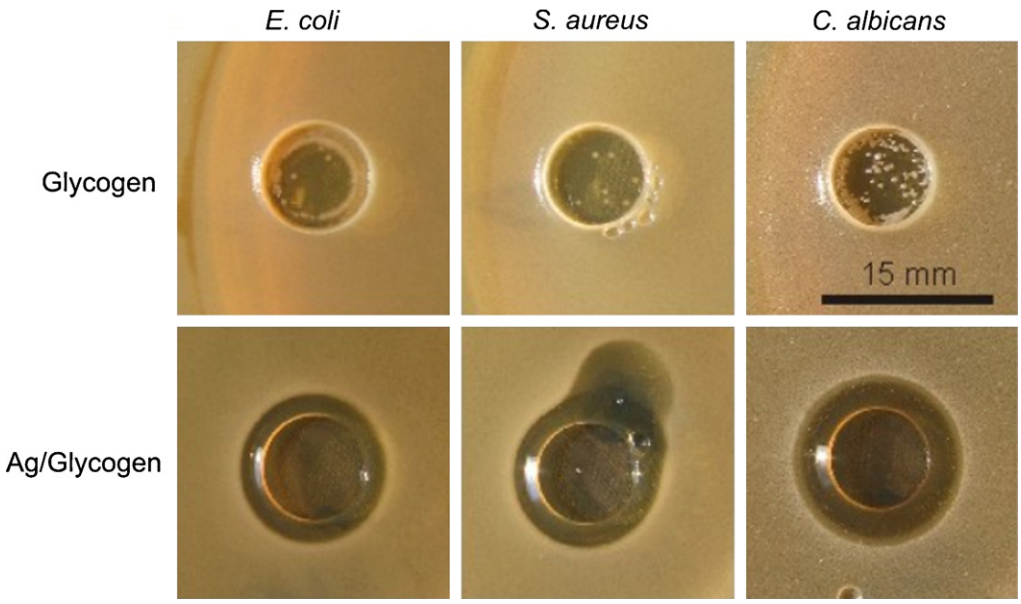

Fig. 7. Antimicrobial test results of glycogen and Ag–glycogen nanocomposite (HP sample) against *E. coli*, *S. aureus* and *C. albicans* obtained by inhibition zone method.

emerges. The fact that the band at 1417 cm^{-1} corresponds to the in-plane vibrations of OH groups (Socrates, 1994) suggests that these groups probably play a key role in the nanoparticles–glycogen interactions. In our previous study on polyvinyl alcohol (PVA)–Ag nanocomposites (Mbhele et al., 2003), we also found that the nanoparticles interacted with the polymer chains via OH groups.

4.3. Antimicrobial activity

Fig. 7 shows typical antimicrobial test results of the pure glycogen and the Ag–glycogen nanocomposites (HP samples) against *E. coli*, *S. aureus* and *C. albicans* obtained by the agar-well diffusion method. While the pure glycogen does not show any clear inhibition zones, the nanocomposite exhibits distinctive effects against all three test microorganisms. The appearance and the size of the clear zone usually depend on the ratio of the circular area and the size of the inoculum, as well as on the solid medium used and the contact area. As can be seen in Fig. 7, the largest inhibition zone of 3 mm is obtained in the case of *C. albicans*. However, the loop samples from this zone showed the growth of *C. albicans*, which indicates that the HP nanocomposites have a fungistatic effect (reduce the number, but not kill completely). On the contrary, the loop samples of the bacterial inhibition zones showed a bactericidal (killing) effect of the HP nanocomposites on *E. coli* and *S. aureus* strains. The results for the MW nanocomposite samples were similar to those obtained for HP samples and for this reason they will not be reported.

In order to further clarify the antimicrobial activity of the Ag–glycogen nanocomposites, the indicator strains were exposed to a given concentration of nanocomposites and after 1 and 2 h of exposure the number of survived cells was measured. The results of the cell count (including controls) and the percent of cells reduction for the MW and HP samples are shown in Table 2. The number of cells of all three microorganisms was significantly reduced after their exposure to the nanocomposites. However, as in the previous tests, the antimicrobial activity of the nanocomposite varied depending on the microorganisms tested. The highest reduction was noticed for *S. aureus* (100.00%), while *C. albicans* was the most resistant. The MW sample was more effective as bactericidal agent to *E. coli*, since it reduces its number by 100.00% after 1 h of exposure. On the other hand, the HP sample was more effective as antifungal agent to *C. albicans*, since its number was reduced by 100.00% after 2 h. In contrast, in the presence of the MW sample the number of *C. albicans* slightly increased after 2 h of exposure ($R = 99.77\%$). The present results show that the glycogen–silver nanocomposites are effective antimicrobial agents with fast activity. Table 2 also shows that the number of cells increased in the presence of the pure glycogen, proving that the antimicrobial activity comes from the nanoparticles. Concerning this result, it is worth mentioning that the Ag–glycogen nanocomposites (films and solutions) stored in air and at room temperature were stable for months after the preparation. At the same time the pure glycogen was completely decomposed.

The effect of different concentrations of silver nanoparticles on the bacterial growth was also studied. The results in Fig. 8 again show that the growth of *C. albicans* was the least affected by the presence of the nanocomposites. The bacterial growth is gradually reduced as the concentration of silver increases and at concentrations above 50 $\mu g\,mL^{-1}$ there was no significant growth for any of the microorganisms (although residuals of *C. albicans* were still

Table 2
Viable cells reduction activity of Ag–glycogen nanocomposites (MW and HP samples) on *E. coli*, *S. aureus* and *C. albicans* after 1 and 2 h of exposure.

Sample	*Staphylococcus aureus*				*Escherichia coli*				*Candida albicans*			
	CFU mL^{-1}		*R*, %		CFU mL^{-1}		*R*, %		CFU mL^{-1}		*R*, %	
	1 h	2 h	1 h	2 h	1 h	2 h	1 h	2 h	1 h	2 h	1 h	2 h
Control	3.8×10^5	6.6×10^5			1.4×10^5	7.5×10^5			3.0×10^4	7.0×10^4		
Contr. Gly	8.8×10^5	9.2×10^5			8.4×10^5	9.6×10^5			3.2×10^5	4.3×10^5		
$HP_{Ag/Gly}$	–	–	100	100	1.0×10^1	–	99.99	100	8.7×10^2	–	99.73	100
$MW_{Ag/Gly}$	–	–	100	100	–	–	100	100	7.6×10^2	1.0×10^3	99.76	99.77

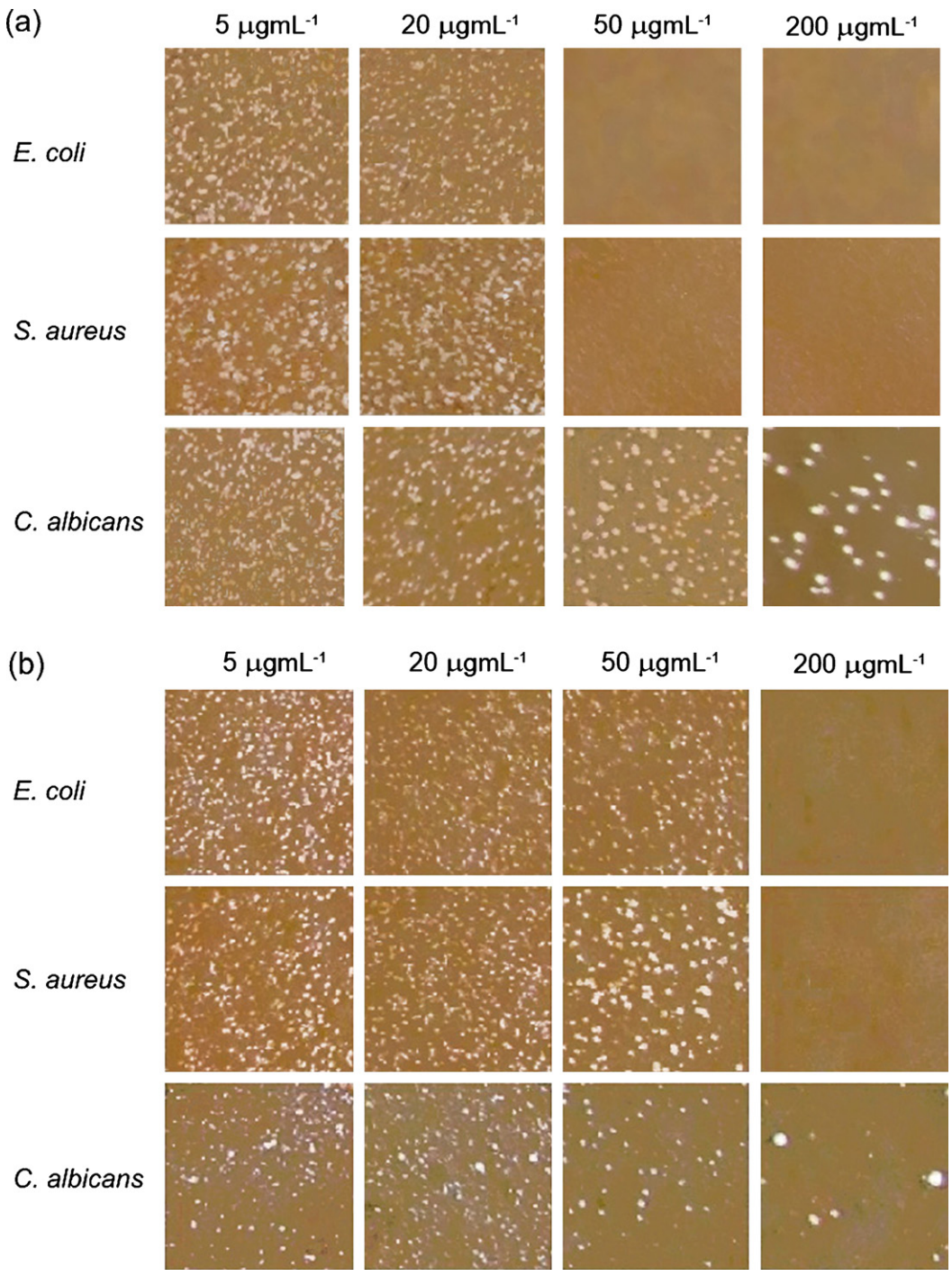

Fig. 8. Microbial growth on agar plates at different concentrations of silver in the nanocomposites; (a) MW and (b) HP nanocomposite samples.

present). It can also be seen that MW sample (Fig. 8a) is more efficient at lower concentrations of silver (20 μg mL^{-1}), especially against *E. coli* and *S. aureus*.

5. Conclusions

The presented results show that glycogen can be regarded as a good stabilization agent for the preparation of silver nanoparticles. At the same time, glycogen can take the role of the matrix of the solid nanocomposite films. The physical properties of the silver–glycogen nanocomposites depended on the mode of preparation. The average sizes of the nanoparticles obtained by MW and HP methods were found to be 9.7 and 10.4 nm, respectively. The samples prepared using microwave radiation showed more distinguished absorption peaks than those prepared by conventional heating. The fluorescence of the glycogen (glycogenin) was found to be partially quenched in the presence of silver nanoparticles. Analysis of the FTIR spectra of the pure glycogen film the nanocomposites suggested that the stabilization of the growth of the silver nanoparticles takes place via glycogen OH groups.

The antimicrobial activity test showed that the degree of inhibition of the microbial growth increases with an increase in silver content. The number of cells is significantly reduced in the presence of silver–glycogen nanocomposite and after 2 h a total reduction

takes place for almost all strains tested. The only exception is the activity of the MW sample against *C. albicans*, where a reduction of 99.77% was observed.

References

Božanić, D. K., Djoković, V., Blanuša, J., Nair, P. S., Georges, M. K., & Radhakrishnan, T. (2007). Preparation and properties of nano-sized Ag and Ag2S particles in biopolymer matrix. *European Physical Journal E*, *22*(1), 51–59.

Božanić, D. K., Djoković, V., Bibić, N., Nair, P. S., Georges, M. K., & Radhakrishnan, T. (2009). Biopolymer-protected CdSe nanoparticles. *Carbohydrate Research*, *344*(17), 2383–2387.

Brayner, R., Vaulay, M. J., Fievet, F., & Coradin, T. (2007). Alginate-mediated growth of Co, Ni, and CoNi nanoparticles: Influence of the biopolymer structure. *Chemistry of Materials*, *19*(5), 1190–1198.

Brown, A. M. (2004). Brain glycogen re-awakened. *Journal of Neurochemistry*, *89*(3), 537–552.

Djoković, V., Krsmanović, R., Božanić, D. K., McPherson, M., Van Tendeloo, G., Nair, P. S., et al. (2009). Adsorption of sulfur onto a surface of silver nanoparticles stabilized with sago starch biopolymer. *Colloids and Surfaces B: Biointerfaces*, *73*(1), 30–35.

Dror-Ehre, A., Mamane, H., Belenkova, T., Markovich, G., & Adin, A. (2009). Silver nanoparticle–*E. coli* colloidal interaction in water and effect on *E. coli* survival. *Journal of Colloid and Interface Science*, *339*(2), 521–526.

Jain, J., Arora, S., Rajwade, J. M., Omray, P., Khandelwal, S., & Paknikar, K. M. (2009). Silver nanoparticles in therapeutics: development of an antimicrobial gel formulation for topical use. *Molecular Pharmaceutics*, *6*(5), 1388–1401.

Kattumuri, V., Katti, K., Bhaskaran, S., Boote, E. J., Casteel, S. W., Fent, G. M., et al. (2007). Gum Arabic as a phytochemical construct for the stabilization of gold nanoparticles: In vivo pharmacokinetics and X-ray-contrast-imaging studies. *Small*, *3*(2), 333–341.

Kvitek, L., Panacek, A., Soukupova, J., Kolar, M., Vecerova, R., Prucek, R., et al. (2008). Effect of surfactants and polymers on stability and antibacterial activity of silver nanoparticles (NPs). *Journal of Physical Chemistry C*, *112*(15), 5825–5834.

Lok, C. N., Ho, C. M., Chen, R., He, Q. Y., Yu, W. Y., Sun, H., et al. (2007). Silver nanoparticles: Partial oxidation and antibacterial activities. *Journal of Biological Inorganic Chemistry*, *12*(4), 527–534.

Manners, D. J. (1991). Recent developments in our understanding of glycogen structure. *Carbohydrate Polymers*, *16*(1), 37–82.

Mbhele, Z. H., Salemane, M., van Sittert, C. G. C. E., Nedeljkovic, J. M., Djokovic, V., & Luyt, A. S. (2003). Fabrication and characterization of silver–polyvinyl alcohol nanocomposites. *Chemistry of Materials*, *15*(26), 5019–5024.

McDonnell, G., & Russell, A. D. (1999). Antiseptics and disinfectants: Activity, action and resistance. *Clinical Microbiology Reviews*, *12*(1), 147.

Melendez, R., Melendez-Hevia, E., & Canela, E. I. (1999). The fractal structure of glycogen: A clever solution to optimize cell metabolism. *Biophysical Journal*, *77*(3), 1327–1332.

Morones, J. R., Elechiguerra, J. L., Camacho, A., Holt, K., Kouri, J. B., Ramirez, J. T., et al. (2005). The bactericidal effect of silver nanoparticles. *Nanotechnology*, *16*(10), 2346–2353.

Murugadoss, A., & Chattopadhyay, A. (2008). A 'green' chitosan–silver nanoparticle composite as a heterogeneous as well as micro-heterogeneous catalyst. *Nanotechnology*, *19*(1), 9.

Pal, A., Esumi, K., & Pal, T. (2005). Preparation of nanosized gold particles in a biopolymer using UV photoactivation. *Journal of Colloid and Interface Science*, *288*(2), 396–401.

Panacek, A., Kvitek, L., Prucek, R., Kolar, M., Vecerova, R., Pizurova, N., et al. (2006). Silver colloid nanoparticles: Synthesis, characterization, and their antibacterial activity. *Journal of Physical Chemistry B*, *110*(33), 16248–16253.

Pirkkalainen, K., Leppanen, K., Vainio, U., Webb, M. A., Elbra, T., Kohout, T., et al. (2008). Nanocomposites of magnetic cobalt nanoparticles and cellulose. *European Physical Journal D*, *49*(3), 333–342.

Radhakrishnan, T., Georges, M. K., Nair, P. S., Luyt, A. S., & Djokovic, V. (2007). Study of sago starch–CdS nanocomposite films: Fabrication, structure, optical and thermal properties. *Journal of Nanoscience and Nanotechnology*, *7*(3), 986–993.

Raveendran, P., Fu, J., & Wallen, S. L. (2003). Completely "green" synthesis and stabilization of metal nanoparticles. *Journal of the American Chemical Society*, *125*(46), 13940–13941.

Rodriguez, P., Munoz-Aguirre, N., Martinez, E. S. M., de la Cruz, G. G., Tomas, S. A., & Angel, O. Z. (2008). Synthesis and spectral properties of starch capped CdS nanoparticles in aqueous solution. *Journal of Crystal Growth*, *310*(1), 160–164.

Romero, J. M., Carrizo, M. E., Montich, G., & Curtino, J. A. (2001). Inactivation and thermal stabilization of glycogenin by linked glycogen. *Biochemical and Biophysical Research Communications*, *289*(1), 69–74.

Sarma, T. K., & Chattopadhyay, A. (2004). Starch-mediated shape-selective synthesis of Au nanoparticles with tunable longitudinal plasmon resonance. *Langmuir*, *20*(9), 3520–3524.

Sharma, V. K., Yngard, R. A., & Lin, Y. (2009). Silver nanoparticles: Green synthesis and their antimicrobial activities. *Advances in Colloid and Interface Science*, *145*(1–2), 83–96.

Socrates, G. (1994). *Infrared and Raman characteristic group frequencies. Tables and charts*. Chichester: John Wiley and Sons.

Sun, C. M., Qu, R. J., Chen, H., Ji, C. N., Wang, C. H., Sun, Y. Z., et al. (2008). Degradation behavior of chitosan chains in the 'green' synthesis of gold nanoparticles. *Carbohydrate Research*, *343*(15), 2595–2599.

Vigneshwaran, N., Kumar, S., Kathe, A. A., Varadarajan, P. V., & Prasad, V. (2006). Functional finishing of cotton fabrics using zinc oxide-soluble starch nanocomposites. *Nanotechnology*, *17*(20), 5087–5095.

Wei, D. W., & Qian, W. P. (2008). Facile synthesis of Ag and Au nanoparticles utilizing chitosan as a mediator agent. *Colloids and Surfaces B: Biointerfaces*, *62*(1), 136–142.

Xiang, M. H., Xu, X., Liu, F., Li, N., & Li, K. A. (2009). Gold nanoparticle based plasmon resonance light-scattering method as a new approach for glycogen–biomacromolecule interactions. *Journal of Physical Chemistry B*, *113*(9), 2734–2738.